JOURNAL OF MATERIALS SCIENCE 19 (1984) 2111–2120

Phenomenology of fracture in sintered alpha silicon carbide

R. K. GOVILA
Ceramic Materials Department, Scientific Research Laboratory, Ford Motor Company, Dearborn, Michigan 48121, USA

Crack propagation mechanisms in a sintered alpha silicon carbide were studied as a function of initial flaw size, temperature, loading rate and applied stress. Surface cracks of controlled size were introduced using the microhardness indentation-induced-flaw (IIF) technique. At room temperature, the fracture stress was found to depend on initial crack size according to the Griffith relationship and extrapolation of the data indicated that processing flaws of 20 to 40 μm were strength controlling. The flexural strength was found to be independent of temperature (20 to 1400° C) and the fracture faces did not show the presence of subcritical crack growth (SCG). Preliminary results from stress rate testing also failed to show the presence of SCG in tests made at 1200° C in air. In contrast, flexural stress rupture tests carried out at 1200 and 1300° C in air using pre-cracked specimens indicated the materials susceptibility to time-dependent deformation and showed the presence of SCG. Fractographic evidence for transgranular crack propagation during fast fracture (catastrophic failure) and intergranular crack propagation during SCG is presented.

1. Introduction

Sintered α-SiC is being investigated for use as structural components for gas turbines and diesel engines. The primary reasons for its use in heat engines are its good oxidation resistance and strength at high temperatures ($\geqslant$ 1000° C), high thermal conductivity and possibly better creep resistance relative to other structural ceramics (e.g. hot-pressed Si_3N_4, sialons, etc). Like many other ceramics, sintered α-SiC is generally regarded as a brittle material with little tolerance, from a structural viewpoint, to incipient flaws (primarily porosity) which are present due to processing and fabrication. The objective of the present work was to determine quantitatively the susceptibility of sintered α-SiC to brittle (catastrophic) fracture and time dependent failure (subcritical crack growth) from inherent flaws and to evaluate the crack propagation mechanisms operative over a temperature range of practical use (1000 to 1400° C). In this paper, we report the results of a series of simple mechanical tests performed on as machined and precracked flexural specimens to measure the bend strength of sintered α-SiC as a function of flaw size, temperature, loading rate and applied stress. In addition, an estimate of the size of strength controlling flaws in the as-processed and machined material, and the fracture energy, γ for brittle failure, have been determined. Fractography is used as the principal interpretive agent for the presence of subcritical crack growth (SCG) and in revealing the mechanistic aspects of crack propagation.

2. Material and experimental techniques

2.1. Material

Sintered α-SiC* was obtained in the form of square billets of approximate dimensions 100 mm x 100 mm x 10 mm. The material was prepared by cold pressing α-SiC powder, followed by sintering at high temperatures, producing a dense (98% theoretical) material with equiaxed α-SiC grains

*Supplied by the Carborundum Company, Niagara Falls, New York, USA.

0022–2461/84 $03.00 + .12

having an average size of 7 to 10 μm. Extremely fine porosity was distributed throughout the microstructure along the grain boundaries as shown later.

2.2. Flexural strength evaluation

For flexural strength evaluation, bend bar specimens of dimension 32 mm long x 6 mm wide x 3 mm thick were machined from the α-SiC billets. All faces were ground lengthwise using a 220 grit diamond wheel and the edges chamfered lengthwise to prevent notch effects. Specimens were tested in 4-point bending in an Instron machine* (Model 1125) at a crosshead speed of 0.5 mm min^{-1} (corresponding to an average stress rate of 1166 MPa min^{-1}) using a specially built self-aligning ceramic fixture [1] made from hot-pressed SiC. The outer and inner knife-edges of the testing fixture were spaced approximately 19 mm and 9.5 mm apart, respectively. The high temperature bend tests were conducted in air in a furnace† attached to the testing machine crosshead. In the high temperature tests, specimens were held at the test temperature for about 15 min to achieve equilibrium before testing was begun. No preload was applied on test specimens for either room temperature or high temperature tests.

2.3. Indentation-induced-flaw technique

Test specimens used in this technique were identical to those used for flexural strength evaluation except that these were precracked using a Knoop microhardness indenter‡ and tested in a similar fashion to the previous specimens. Indenting the sintered α-SiC with a Knoop indenter resulted in the introduction of surface cracks whose geometry and size (depth of crack) were controlled by the choice of indenter load. At indentation loads up to 4000 g ($\sim$ 39.2 N), the crack fronts were semi-circular in geometry although at this higher indentation load, the depth of crack varied considerably. A schematic representation of crack geometry in a test specimen and details about the indentation-induced-flaw (IIF) technique have been reviewed earlier [2–5]. All precracking was done at room temperature.

2.4. Stress-rate testing

Machined flexural specimens were used in this technique to generate data on fracture stress as a function of stressing rate at 1200° C in air. Specimens were tested over two orders of magnitude of stressing rate using crosshead speeds of 0.5, 0.05 and 0.005 mm min^{-1} (corresponding to an average stress rate of 1166, 104 and 11 MPa min^{-1}, respectively). A total of 3 or 4 specimens were tested at a given machine crosshead speed. The individual stress-rates were calculated from the linear (elastic) portion of the load-deflection curve and an average value of the stress rate was used.

2.5. Flexural stress rupture evaluation

Precracked specimens containing cracks of two different depths (4000 g and 2000 g microhardness Knoop identation load) were used for stress rupture testing and the tests at high temperatures (1200 to 1400° C) were conducted in four-point bending using the self-aligning ceramic fixture and high temperature furnace. The load was applied on the test specimen through a cantilever arm with a dead-weight. The experimental set-up was equipped with a microswitch to cut off power supply to the furnace and the timer at the instant failure of the specimen occurred and the total time-to-failure was recorded. The temperature was allowed to stabilize for a minimum of 30 min before full load was applied. During preheating of the furnace, the specimen was subjected to a small stress ($\sim$ 34 MPa) due to the combined weights of cooling jacket and lever arm assembly. Details of the test set-up are given elsewhere [6].

3. Results and discussion

3.1. Fracture energy and flaw-size estimate

A series of specimens was prepared and precracked with microhardness indentation loads ranging from 1000 to 4000 g. The variation of fracture stress with crack depth (as measured optically from the fracture face) for sintered α-SiC specimens tested at 20° C is shown in Fig. 1, and the data§ show a linear variation consistent with the Griffith [7] criterion for brittle fracture:

$$\sigma_F \approx Y[E\gamma/c]^{1/2} \quad (1)$$

*Supplied by the Instron Corp., Canton, Massachussetts, USA.
†Supplied by CM Inc., High Temperature Furnaces, Bloomfield, New Jersey, USA.
‡Supplied by Wilson Instrument Div., ACCO, Bridgeport, Connecticut, USA.
§Individual fracture strengths and the corresponding crack depths are given in Table I (see later).

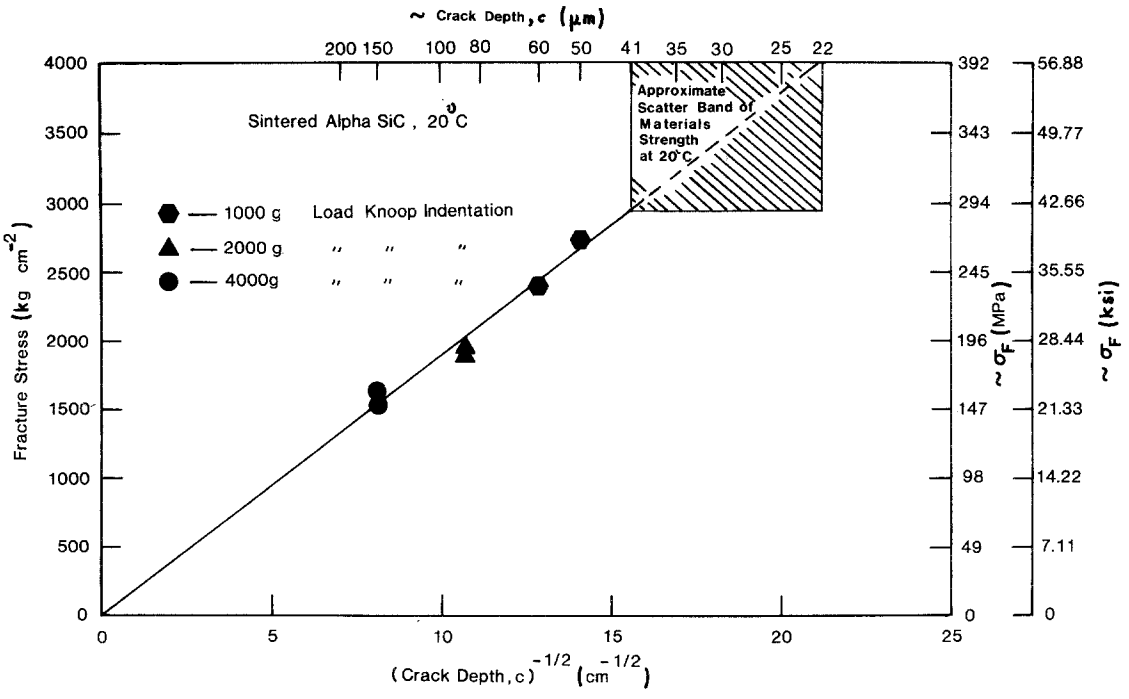

Figure 1 Variation of fracture stress as a function of inverse square root of crack depth at room temperature.

where σ_F is the fracture stress required to propagate a pre-existing crack of known dimensions, Y is a constant relating primarily to crack geometry and specimen dimensions, E is Young's modulus, c is the initial crack depth at which fracture initiated, and γ is the fracture energy. For approximately semi-circular cracks (as shown later) and for simplicity, Y is taken as unity. For a value of $E \approx 406$ GPa* at room temperature and the slope of the curve shown in Fig. 1, the computed value of fracture energy, γ, is ~ 8.5 J m^{-2} (8500 ergs cm^{-2}) at 20° C. It is imperative to note, however, that the above can be taken rigorously only as a demonstration of principle. The presence of residual stresses (tensile at the crack front) at microhardness indentation sites has been suggested by several investigators as discussed elsewhere [2–5]. It is important to realize that the presence of such stresses could significantly influence the absolute magnitude of the experimentally determined fracture energy.

The most useful application of the data shown in Fig. 1 is as a means of estimating the flaw size in machined sintered α-SiC. Extrapolation of the data in Fig. 1 to the fracture stress of uncracked (machined) test samples (shown as the approximate scatter band of materials strength) indicates that flaws of the order of 20 to 40 μm in size are present in the as processed sintered α-SiC. This theoretical prediction about the flaw size was in fact confirmed in several test specimens where failure origins and randomly occurring flaws in the material were close to the predicted size as typically shown in Fig. 2, for two different specimens tested at 20° C. To date, this is perhaps the best estimate of the flaw size in sintered α-SiC. Many investigations [8–12] of mechanical properties and fracture mechanics aspects of sintered α-SiC are on record but none reported an attempt to measure or estimate the processing flaw size.

3.2. Flexural strength against temperature

Fifteen bend bar specimens were tested at room temperature in order to determine the mean strength and the Weibull modulus. The material showed a large scatter in σ_F possibly due to large variations in processing flaw sizes. The σ_F varied from a minimum of 289 MPa to a maximum of 390 MPa with a distribution mean of 337 MPa, standard deviation of 37 MPa and Weibull modulus, $m \approx 11$. Two types of porosity were observed in the bulk material on the fracture faces of specimens, see Fig. 2: Fine pores usually of the size 0.5 to 3 μm distributed uniformly along the grain

*Taken from Manufacturers Technical Information Sheet (Carborundum Co.).

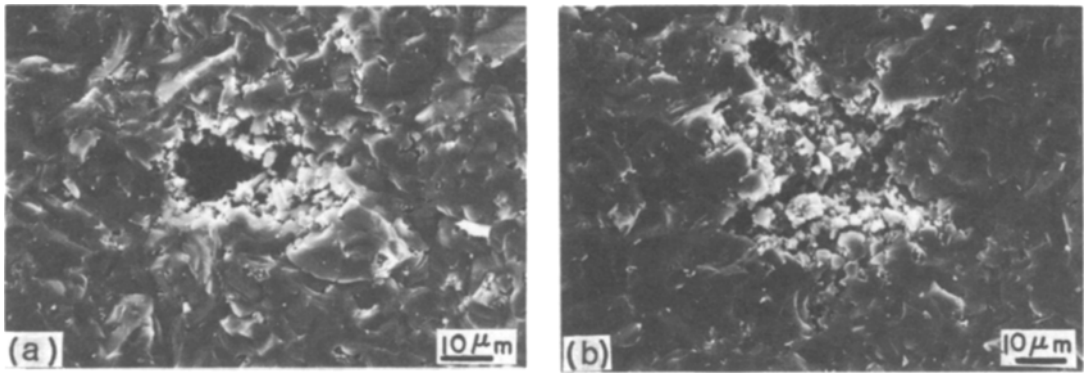

Figure 2 Typical porosity as seen in SEM on the fracture faces of sintered α-SiC specimen tested in flexure at 20° C.

boundaries and large pores usually of the size 20 to 80 μm. Failure occurred in a brittle (catastrophic) manner and the majority of the failure initiation sites were associated with porosity both surface and subsurface, see Fig. 3.

Flexural strength was also evaluated at higher temperatures (800 to 1400° C) in order to determine if any micro-plastic deformation accompanied the fracture process and if subcritical (slow) crack growth (SCG) occurs. The variation in fracture strength as a function of temperature is shown in Fig. 4. There is considerable scatter in the data, both in tests made at 20° C and higher temperatures (800 to 1400° C). However, it should be noted that the mean strength for the two sets of data* are the same. Therefore, the flexural strength,

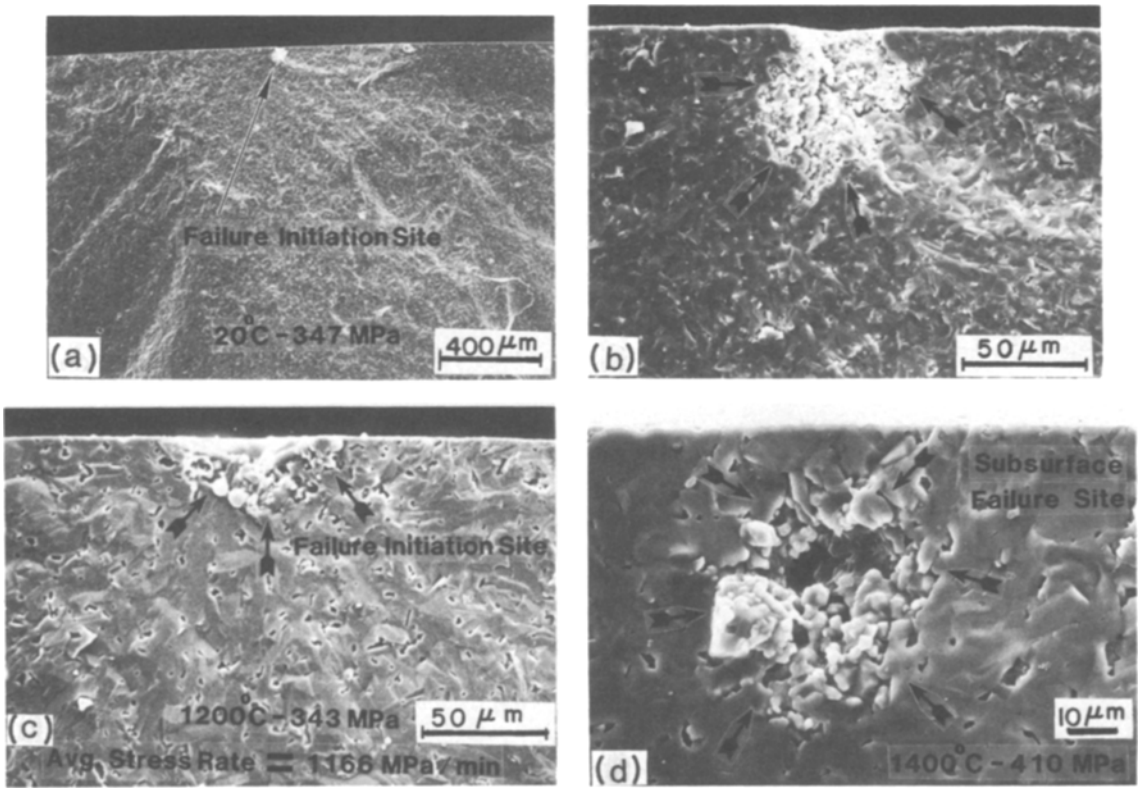

Figure 3 SEM fractographs showing failure sites in sintered α-SiC specimens tested in flexure. All the above specimens were tested at the crosshead speed of 0.5 mm min^{-1}.

*A total of 15 and 13 specimens were tested at 20° C and higher temperatures (800 to 1400° C), respectively. Individual fracture strength values are given in [6].

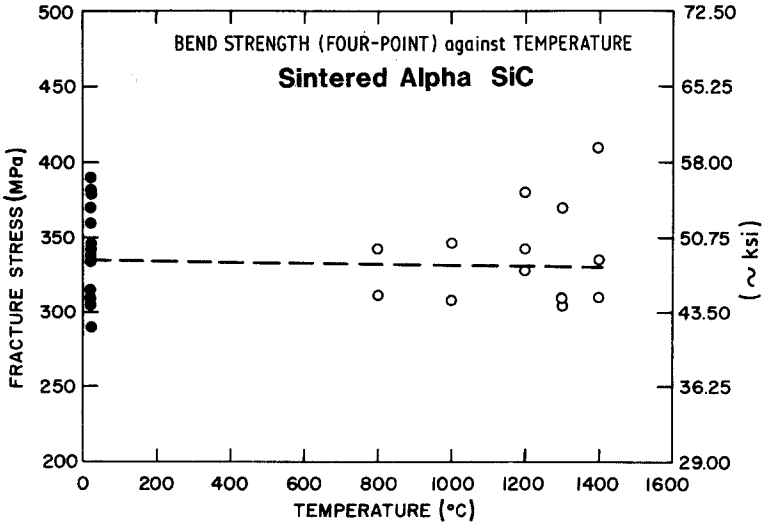

Figure 4 Variation in fracture strength as a function of temperature.

σ_F, is shown as constant and independent of temperature, Fig. 4. The fracture surfaces at higher temperatures (1200 to 1400° C) were similar to that observed at 20° C, Figs. 3c and d, and did not show any signs of SCG. In all these tests, all fracture faces showed a smooth appearance characteristic of fast fracture similar to cleavage of ionic single crystals and this type of failure is characterized by transgranular crack propagation, Figs. 3b, c and d. In short, the flexural strength evaluation indicates the absence of SCG up to about 1400° C and the primary mode of fracture during crack propagation is transgranular.

3.3. Stress rate measurements

The presence of subcritical crack growth in ceramic materials can be described by the functional relationship between crack velocity, V, and stress intensity factor, K_I, as follows:

$$V = AK_I^n \qquad (2)$$

where A and n are constants. Flexural stress rate testing [13–15] is one simple method for determining the crack propagation parameter, n, and utilizes the materials fracture strength as a function of stressing rate as shown below for a given temperature and environment:

$$\sigma_F = D\dot{\sigma}_F^{1/(n+1)}$$

or

$$\log \sigma_F = \log D + \frac{1}{(n+1)} \log \dot{\sigma}_F \qquad (3)$$

where σ_F is the fracture stress at a stressing rate of $\dot{\sigma}_F$ and D is a constant. The fracture stress variation as a function of stressing rate for sintered α-SiC at 1200° C in air is shown in Fig. 5. A large scatter in experimental data is visible and suggests the absence of stress rate dependence on the fracture stress. The inclined line as drawn could easily be drawn as horizontal. The slope of the line yields an n value of 47 at 1200° C. The smaller the value of n, the greater the tendency for SCG to occur. The large value of n measured here strongly suggests the absence of SCG in this material at 1200° C. This view was further confirmed when the fracture faces of specimens tested

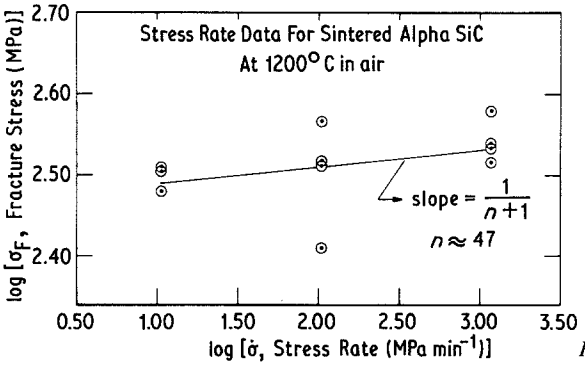

Figure 5 Fracture stress vs stressing rate of sintered α-SiC.

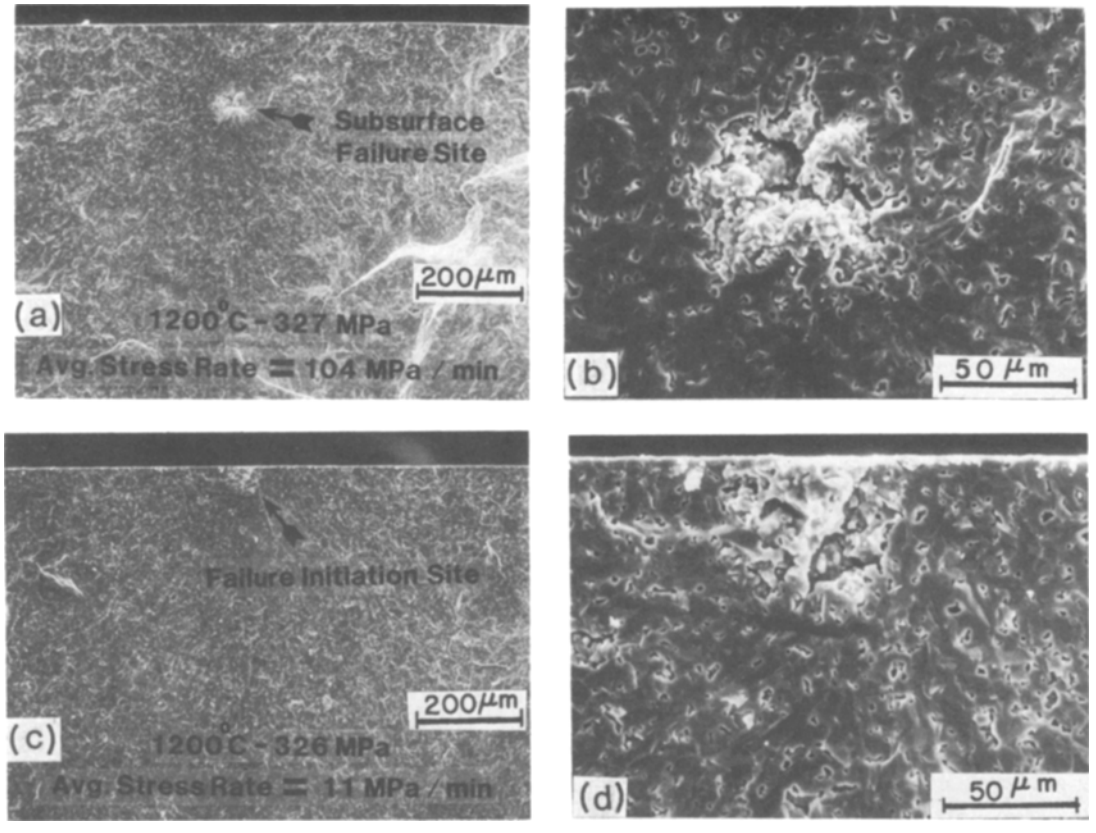

Figure 6 SEM fractographs of sintered α-SiC specimens tested in flexure at 1200° C in air as a function of stressing rate. (a) Specimen tested at a crosshead speed of 0.05 mm min^{-1}. (b) Higher magnification view of failure site seen in (a) showing porosity. (c) Specimen tested at a crosshead speed of 0.005 mm/min. (d) Higher magnification view of failure site seen in (c). Note, these fractographs show essentially the same fracture mode (fast fracture-transgranular crack propagation) as that seen in Fig. 3, and no signs of slow crack growth are visible.

at extremely slow crosshead speeds (0.005 mm min^{-1}, corresponding to an average stress rate of 11 MPa min^{-1}) failed to show the presence of SCG, see Fig. 6. Also, the load–deflection curves for this material tested at the lowest stressing rate of 11 MPa min^{-1} (or a crosshead speed of 0.005 mm min^{-1}) showed a smooth behaviour and did not show any load drops, Fig. 7, which typically suggest localized crack growth due to viscous flow.

In contrast, similar stress rate studies were made by McHenry and Tressler [10] in this material at 1000° C in both the presence (10^{-4} atm p_{O_2}) and absence (10^{-8} atm p_{O_2}) of an oxygen environment. The unoxidized material showed stress rate independence while oxidized samples showed stress rate dependence with an n value of 41 at 1000° C. Since their load–deflection curve at the lowest stressing rate (corresponding to the crosshead speed of 0.005 mm min^{-1}) showed load drops occurring over 1 to 2 min time span, the authors inferred the occurrence of SCG. There was, however, no fractographic evidence presented of SCG. The sensitivity of the stress rate method* to other factors may, therefore, preclude the unambiguous identification of SCG by this technique – for example, the presence of large size processing flaws (porosity) can act as stress raisers and lead to early failures. Secondly, the test temperature of 1200° C in air may be the borderline temperature (transition temperature) and not high enough to induce SCG prior to fast failure. In addition, the total time to failure at the slowest stress rate of 11 MPa min^{-1} (crosshead speed 0.005 mm min^{-1}) used, was of the order of 60 min and this may

*It should be pointed out that the stress rate method clearly reveals fractographically the presence of SCG in many other ceramic materials such as soda-lime glass, etc. It is not the author's intent to imply that the method is not useful.

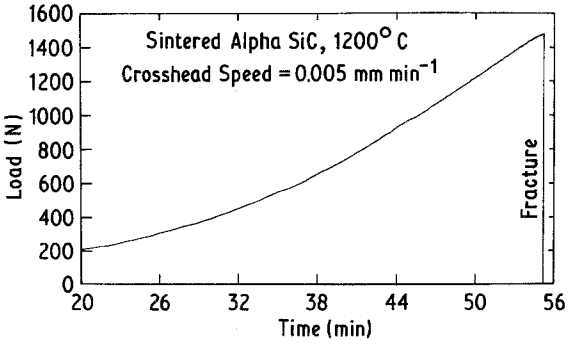

Figure 7 Trace of load-deflection curve for sintered α-SiC (four-point bending) specimen tested at 1200° C in air at a crosshead speed of 0.005 mm min^{-1} (corresponding to an approximate stress rate of 11 MPa min^{-1}) and the fracture surface is shown in Fig. 6 (c and d).

not be sufficient to induce SCG in this material. Therefore, stress rate tests should be carried out at higher temperatures (≥ 1300° C in air) to determine if this method is sensitive enough to conclusively reveal fractographically the presence of SCG in sintered α-SiC.

3.4. Flexural stress rupture evaluation

Flexural stress rupture studies have been made in detail on the machined specimens of sintered α-SiC at 1200° C in air by Quinn and Katz [16] and Quinn [17] and they concluded, on the basis of quantitative estimates (using a $\log \sigma_F$ against $\log t_F$ time-to-failure plot and determining the crack propagation parameter, n), that the material showed time-dependent failure or slow crack growth (SCG). However, in both studies [16, 17] the fracture surfaces failed to show the presence of SCG (even those specimens which sustained the applied stress for ≥ 500 h) and appeared similar to the fast fracture surface at 20° C. Stress rupture studies have been carried out here on α-SiC to determine if SCG can be unambiguously identified by fractographic techniques. In this investigation the stress rupture studies were concentrated at 1200° C in air. The use of precracked specimens in revealing the occurrence of SCG at a given temperature and applied stress has been successful in several ceramic materials [18, 19]. The precracked specimen contains a localized stress concentration site (a semi-circular type region) and therefore, all the resulting micro-plastic deformation leading to SCG will be concentrated along the boundary of the crack front. This facilitates fractographic examination to identify SCG since the occurrence is confined to this well identified region.

A series of bend bar specimens was precracked using a Knoop microhardness indenter with either 4000 g (39.23 N) or 2000 g (19.61 N) indentation load, giving two different depths of crack. The specimens were stressed to a fraction of the room temperature fracture strength (see Table I) at 1200° C in air, and the applied stress was maintained for a given length of time; afterwards the applied stress was increased. Finally if failure did not occur within a reasonable time (≤ 20 h), the test specimen was unloaded and broken in 3-point bending at 20° C to reveal any SCG or deformation which may have occurred along the crack front boundary. The results are summarized in Table I. Specimens containing large cracks (approximately 130 to 160 μm deep, precracking load 4000 g) and subjected to applied stresses varying from 107 MPa to 168 MPa at 1200° C, did not exhibit any evidence of SCG in a limited time frame (see Table I). It should be pointed out that subcritical crack growth is primarily dependent on (a) test temperature, (b) applied stress (c) environment (water, vacuum, salt solutions, etc.) and (d) composition of the material (impurities) or additives added in order to promote sintering or hot-pressing). It is a combination of these factors which promotes or induces SCG. In this study, only subcritical crack growth as influenced by test temperature and applied stress in air environment is discussed.

The extreme importance of temperature in inducing SCG is well illustrated when similar precracked specimens containing large cracks (130 to 160 μm deep) were tested in flexural stress rupture mode at 1300° C, Table I. This is illustrated by the specimen tested at an applied stress of 112 MPa for 46 h, unloaded and broken in 3-point bending at 20° C to reveal the initiation of SCG along the crack front, ACB. The start of SCG in the vicinity of location 'A' is visible, Fig. 8. Note, that a similar type precracked specimen (specimen 8, Table I) tested at the same applied stress, 112 MPa, failed to reveal any occurrence of SCG at 1200° C after over 100 h. This immediately suggests that the initial crack size (130 to 160 μm) is slightly too large for SCG to occur at 1200° C and possibly a combination of smaller crack size and slightly increased applied stress would induce the occurrence of SCG at 1200° C. As the applied stress was increased in tests at 1300° C, the

TABLE I Flexural strength and stress rupture results for precracked (Knoop indented) sintered α-SiC specimens

Test number	Test temperature (° C)	Indentation load (g)	Approximate crack depth (μm)	Fracture stress at 20° C (MPa)	Applied stress (MPa)	Time (h)	Remarks
1	20	1000	60	235	–	–	Failed at the crack site
2			50	268	–	–	Failed at the crack site
3		2000	88	187	–	–	Failed at the crack site
4			88	191	–	–	Failed at the crack site
5		4000	150	149	–	–	Failed at the crack site
6			150	159	–	–	Failed at the crack site
7	1200	4000	–	335*	107	163	Unloaded, failed at the crack and did not show SCG
8			135–140	329*	112	100	Unloaded, failed at the
					152	70	crack and did not show SCG
9			130–135	290*	137	48	Unloaded, failed at the
					168	20	crack and did not show SCG
10			–	–	137		Failed instantly at the crack site. No SCG
11			–	–	168		Failed instantly at the crack site. No SCG
12		2000	–	–	137	300	Unloaded, did not fail at the crack site
13			88	294*	150	144	Unloaded, failed at the crack site and showed SCG (see Fig. 10)
14			88	–	175	10	Failed at the crack and showed SCG
15			88	–	195		Failed instantly. No SCG
16	1300	4000	160	263*	112	46	Unloaded, failed at the crack site and showed initiation of SCG (see Fig. 8)
17			150	267*	137	45	Unloaded, failed at the
					146	25	crack site and showed initiation of SCG (see Fig. 9)
18			150–155	–	155	19	Failed at the crack and showed SCG

*In 3-point bending.

initiation of SCG along the crack front ACB was clearly visible, Fig. 9. The mode of fracture during SCG is primarily intergranular, Fig. 9b. Note that the fracture surface morphology inside the precrack (ACB) region, and outside the SCG band (EDF) is similar and indicative of fast fracture, characterizing a transgranular crack propagation mode.

To test the importance of initial crack size and applied stress on SCG, precracked specimens containing a smaller size crack (85 to 90 μm deep, 2000 g Knoop indentation load) were tested in stress rupture at 1200° C in air, and the results are given in Table I. The first specimen was subjected to 137 MPa at 1200° C in air and sustained the load for 300 h without failure. The specimen was unloaded and broken in 3-point bending at 20° C to reveal the extent of deformation (SCG) at the crack front. The specimen did not fail at the precrack site, possibly due to crack blunting and broken elsewhere at a surface pore. In another test, the applied stress was increased to 150 MPa and the specimen sustained the stress for 144 h without failure. The specimen was unloaded, broken in 3-point bending at 20° C, failed at the precrack site, and showed the occurrence of SCG along the crack front boundary, Fig. 10. The SCG band as seen at 1200° C, Fig. 10a, is similar in

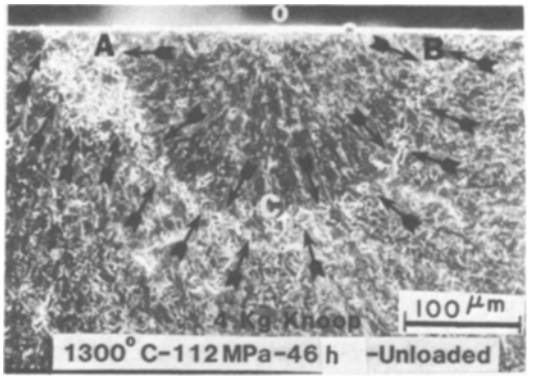

Figure 8 SEM fracture surface of a precracked sintered α-SiC specimen tested in flexural stress rupture mode at 1300° C, unloaded and broken in 3-point bending at 20° C. ACB is the semi-circular precracked (CO ≈ 160 μm deep) region. Limited slow crack growth occurred in the vicinity of A and along the crack front boundary ACB as indicated by the arrows.

its appearance to that seen at 1300° C (Fig. 9a) and the morphology of crack propagation during SCG is largely intergranular, Fig. 10b. Increased applied stress levels led to early failure, Table I. Similar flexural stress rupture studies have been carried out at 1300 and 1400° C in machined specimens [6] of sintered α-SiC in order to identify the stress limits for a reasonable time (≤ 100 h) without showing signs of degradation of strength due to the presence of SCG.

The overall conclusion of these stress rupture studies relative to SCG is that fracture can involve SCG at temperatures as low as 1200° C. However, fracture can also take place directly from the inherent flaw with no SCG development. It appears that the occurrence or absence of SCG is a sensitive function of the inherent flaw size and shape, temperature and applied stress.

4. Summary

At room temperature, the fracture stress was dependent on crack length according to the Griffith criterion. Extrapolation of the data indicated that processing flaws (porosity) of ≈ 20 to 40 μm were responsible for brittle fracture of sintered α-SiC material. The fracture surface energy, γ, calculated at 20° C for fast fracture is about 8.5 J m^{-2}.

The flexural strength was found to be independent of temperature (20 to 1400° C) and the material did not show the occurrence of subcritical crack growth. Failure occurred in a brittle manner and the mode of crack propagation during fast fracture was primarily transgranular. The stress rate data obtained at 1200° C in air showed large scatter suggesting the absence of a stressing rate dependence on the fracture stress, and the fracture surfaces failed to show the presence of subcritical crack growth.

Flexural stress rupture testing at 1200° C in air using precracked specimens of sintered α-SiC showed the initiation of subcritical crack growth (SCG). The extent of SCG increases with increasing temperature. The mode of crack propagation during SCG was primarily intergranular.

Acknowledgements

The author thanks Dr T. J. Whalen and Dr Peter Beardmore for reviewing the paper and R. Goss for

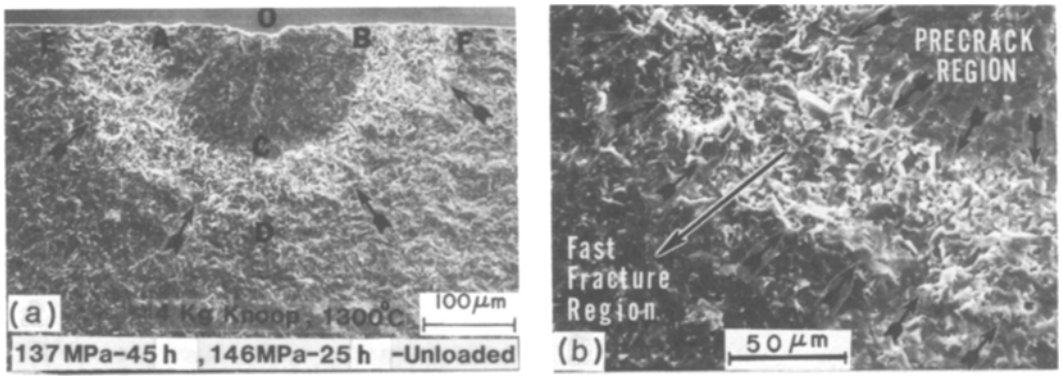

Figure 9 SEM fracture surface of a precracked sintered α-SiC specimen tested in flexural stress rupture mode. (a) ACB is the semi-circular precracked region. The white band surrounding ACB is the slow crack growth region whose boundary is marked by the arrows. (b) Higher magnification view along the path AC seen in (a). Long arrow indicates the direction of crack propagation and the transition from intergranular crack growth to fast fracture (transgranular crack propagation).

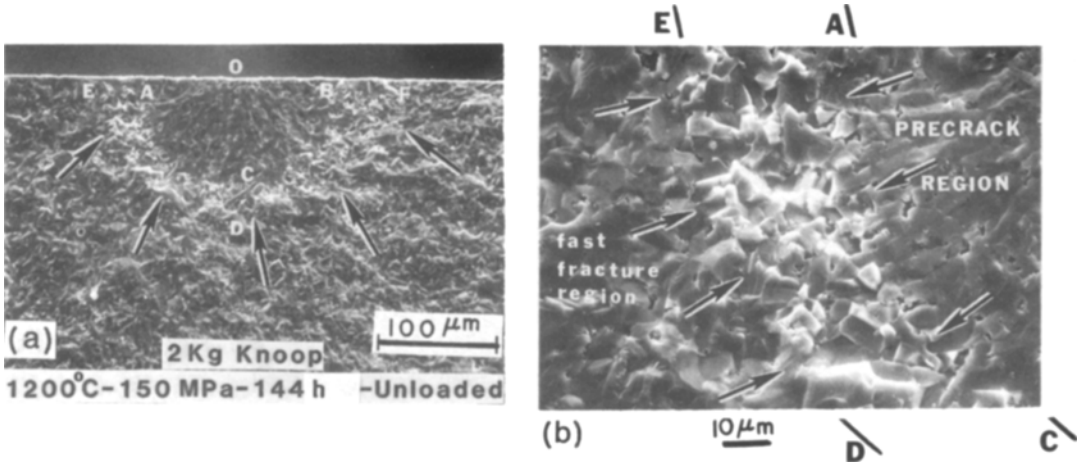

Figure 10 SEM fracture surface of a precracked sintered α-SiC specimen tested in flexural stress rupture. (a) Precracked region ACB is surrounded by the white band as the slow crack growth region. (b) Higher magnification view of the white band region along EACD path. Slow crack growth occurs by intergranular crack propagation while fast failure region shows transgranular crack propagation.

SEM work. This work was supported in part by the Department of Energy under Contract No. DAAG-46-77-C-0028, monitored by Dr E. M. Lenoe, Army Materials and Mechanics Research Center, Watertown, Mass.

References

1. R. K. GOVILA, AMMRC Technical Report 80-18, May, 1980.
2. R. K. GOVILA, *J. Amer. Ceram. Soc.* **63** (1980) 319.
3. B. R. LAWN, A. G. EVANS and D. B. MARSHALL, *ibid.* **63** (1980) 574.
4. G. R. ANSTIS, P. CHANTIKUL, B. R. LAWN and D. B. MARSHALL, *ibid.* **64** (1981) 533.
5. P. CHANTIKUL, G. R. ANSTIS, B. R. LAWN and D. B. MARSHALL, *ibid.* **64** (1981) 539.
6. R. K. GOVILA, "High Temperature Strength Characterization of Sintered Alpha Silicon Carbide," Tech. Rept. AMMRC TR 82-51, October, 1982.
7. A. A. GRIFFITH, *Phil. Trans. R. Soc. London A* **221** (1920) 163.
8. E. H. KRAFT and R. H. SMOAK, in "Proceedings of the Fall Meeting of the American Ceramic Society," Hyannis, Mass., Sept. 28, 1977.
9. G. D. QUINN, AMMRC Technical Report 80-15, April, 1980.
10. K. D. McHENRY and R. E. TRESSLER, *Amer. Ceram. Soc. Bull.* **59** (1980) 459.
11. S. G. SESHADRI and M. SRINIVASAN, *J. Amer. Ceram. Soc.* **64** (1981) C69.
12. J. A. COSTELLO and R. E. TRESSLER, *ibid.* **64** (1981) 327.
13. R. J. CHARLES, *J. Appl. Phys.* **29** (1958) 1549.
14. R. J. CHARLES, *ibid.* **29** (1958) 1657.
15. F. F. LANGE, *J. Amer. Ceram. Soc.* **57** (1974) 84.
16. G. QUINN and R. N. KATZ, *ibid.* **63** (1980) 117.
17. G. QUINN, AMMRC TN 81-4, Dec., 1981.
18. R. K. GOVILA, K. R. KINSMAN and P. BEARDMORE, *J. Mater. Sci.* **13** (1978) 2081.
19. *Idem, ibid.* **14** (1979) 1095.

Received 10 June
and accepted 19 September 1983